Appendix A

The Analysis of shower images

In the first chapter, concerning theory and detectors, I gave a short overview of γ^1-rays from their production in the source up to their development as air showers and their detection by Cherenkov telescopes. A much higher quantity of hadronic particles impinge onto the earth's atmosphere than γ-**rays**, which themselves only account for **less than 0.1%** of all cosmic rays. One of the main challenges of γ-astronomy is therefore the separation of γ's from the hadronic background. A **certain** gamma/hadron separation is already applied by the **telescope trigger**, which only responds to signals in a limited time window and takes advantage of the fact that Cherenkov photons from hadronic showers arrive with a **larger time spread** and have a lower light yield for the same energy as compared to γ's. From the moment that they have been recorded and measured in the form of Cherenkov images, the key issue becomes to **separate** gamma shower events from hadronic shower events as efficiently as possible.

The data used in this chapter are a part of the complete dataset of Mkn 421 from February to May 2001 and account for approximately **167 hours** of observation time (from a total of 250 hours that will be analyzed in the last chapter). It was recorded by the **CT1** telescope of the HEGRA collaboration on La Palma on the Roque de los Muchachos. The data has been preprocessed by a filter and the preproc-program written by Dirk Petry of the Max Planck Institut für Physik in Munich. The filter checks the data for some simple errors in mainly two ways: a) **rejection of noise triggered events** by applying a two next neighbor software-trigger and b) checks for **correct positioning** of the telescope. After the filter cuts, the trigger rate in zenith position is approximately 2.6 Hz to 3 Hz. Then, the preprocessing program which does the **calibration** is applied. It converts the signal into photoelectrons for each pixel and determines their pedestal RMS values from calibration runs. The next steps are done by a software package written in **C++/ROOT** which consists of about 50.000 lines of code that I developed. The software reads the calibrated data output and perform all the algorithms and analysis procedures discussed in this chapter.

For telescope efficiency studies, flux calculations and energy calibrations, Monte Carlo (MC) studies are essential. The MC simulation of air showers plus their imaging on the telescope have been done by Dorotha Sobczynska of the University of Lodz in Poland.

In the shower and telescope simulation by Dorotha Sobczynska the simulation of the night sky background (NSB) is not included and must be performed separately for each source analyzed. Therefore the **simulation of the NSB** is done within the program package developed for this work and will be described in the following sections.

This chapter is structured in the following way. After a quick description of the **calibration procedure** of preproc, an overview of the **Monte-Carlo simulation** is given. The next section deals with the **classical image parameters** and various **separation methods** (for instance, **static cuts**, **dynamic cuts** and a **modified linear discriminant method** (LDA))

---

[1]Note: Throughout this document the abbreviation 'γ' refers to a high energy photon (>1 GeV)

which are used to quantify the discriminating power of a given image parameter set. **New image parameters** are introduced and classified by using the **LDA**. In the last section the **estimation of energy**, **pointing corrections**[2], **unfolding of spectra, flux calculations** and determination of the **integrated light flux** (above 1 TeV -> light curve) will be discussed.

A.1 The calibration of the telescope data

Here I wish to briefly discuss how the raw data from the CT1-telescope is calibrated. The calibration is done via a software 'preproc' which was written by Dirk Petry of the Max Planck Institut für Physik in Munich and significantly modified and improved by Martin Kestel, also in Munich. It directly reads the recorded rawdata of the telescope, which consists of **pedestal runs**, **calibration runs** and **observation runs**. The data simply consists of the ADC-values of each pixel that is recorded when a trigger occurs.

During pedestal runs random trigger images of the sky at the position of a source are taken. As the name implies, they are used to determine the pedestal position (in ADC counts), which means the zero line, and its RMS value of the pedestal peak. The RMS value is a measure of the light of the night sky and is proportional to the square-root of the PMT current. This will be explained in more detail in the next section concerning Monte Carlo simulation.

The calibration runs consist of a train of LED light-pulser events of equal amplitude. From the position of the signal peak, its RMS and the position of the pedestal, **the number of photoelectrons** can be calculated using the so-called **excess noise factor method** [Mir00, Sch01].

$$N_{PhE} = F \frac{(\mu - \mu_0)^2}{\sigma^2 - \sigma_0^2} \tag{A.1}$$

where μ and μ_0 are the signal and pedestal position and σ and σ_0 are the standard deviations of the signal peak and the pedestal peak. By assuming that N_{PhE} is equal for each pixel (so-called flat-fielding) and by knowing the average excess noise factor for all PMTs in the camera a **conversion factor** for ADC-channels->PhE for each pixel is calculated.

The precision of this method is estimated to be approximately 10 % [MirCom]. The conversion factors are calculated by evaluating the calibration and pedestal runs. Once the conversion factors are known they are used by the 'preproc' program to **determine the number of PhE** for each pixel of all the events in an observation run.

A.2 Monte Carlo Simulation of air showers

The Monte Carlo (MC) simulation of air showers and their imaging on the telescope camera is a very important part of the analysis, since it helps to understand the difference between gamma showers and hadronic showers. The simulation of the trigger of the telescope and the imaging of the shower onto the focal plane are absolutely mandatory to calculate the **cut and trigger efficiencies**, which ultimately determine the **effective areas** after cuts and the flux. The **energy calibration** of the data is done by using MC data. This is done by first finding a good estimation of the shower energy of MC gamma showers and then applying this result to real data. This topic will be discussed later on.

The showers have been simulated by a base program from the Max Planck Institut in Karlsruhe/Germany called **CORSICA** which uses experimentally determined cross sections and complex atmospheric models to simulate the extended air showers by tracking each particle in the shower individually. As mentioned above, the simulation of the showers and especially the telescope reflector simulation have been performed by Dorotha

---

[2]The word 'mispointing' is used in the sense that the center of the camera does not coincide exactly with the coordinates of the object to which the telescope is pointing to. A 'pointing correction' corrects the data for slight misalignments.

Sobczynska. For the imaging onto the camera, the exact mirror and camera geometry have been taken into account, including optical imperfections. To obtain good agreement with the real measurement, the influence of the **night sky background** (NSB) and the light of starfields also need to be simulated. This is explained in the following section.

A.2.1 Simulation of the night sky light

In between to the normal data taking runs (for the observation of an astronomical object), **calibration runs** and **pedestal run**s are also performed. The calibration runs are used to determine the **conversion factor** of ADC-channel/PhE. The pedestal runs consist of images of the night sky using random triggers to ensure the exclusion of shower light. The pedestal runs are used to measure the **zero line** of the ADC (pedestal) and its **RM**S. The pedestal RMS of each pixel is calculated by taking the variance of the measured signal in each pixel. Both, the electronic noise and the light of the night sky (NSB) including starlight, contribute to the RMS. The NSB accounts to approximately 0.8-3 PhE per pixel (depending on observation conditions) within the time window of the ADC (approximately 30 ns).

To understand the **shape** of the resulting pedestal distribution, which we want to simulate, it is necessary to understand the camera electronics in significant detail. The light is recorded by PMTs which have a photocathode which converts photons into photoelectrons with a certain QE. The signal seen at the output of the PMT is the amplified signal of the PhEs hitting the first dynode. The number of PhE within the time window of the ADC is Poisson distributed. The further amplification has fluctuations due to its statistical nature. The dominant contribution comes from the first dynode. This **additional noise is called excess noise** (**F**). For PMTs it is defined as

$$F^2 = 1 + \frac{var(Single\,PhE\,Peak)}{mean^2(Single\,PhE\,Peak)} \tag{A.2}$$

The definition of F simply describes the increase of the noise of an incoming signal after amplification through the dynode system of a PMT. More generally (for any type of amplifier):

$$F^2 = \frac{Signal_{input}^2 / \left(\sigma_{input}^2 - \sigma_{el}^2 \right)}{Signal_{output}^2 / \left(\sigma_{output}^2 - \sigma_{el}^2 \right)} \tag{A.3}$$

The noise at the input and at the output is understood as noise without the electronic noise of the amplifier $\sigma^2 = \sigma_{real}^2 - \sigma_{el}^2$. In the simulation the **Poisson distributed signal** of the PhE, with mean λ, has to be **folded** with a **Gaussian distribution** (coming from excess noise and electronic noise). The output signal of the PMT (the gain has been normalized to one) is then:

$$f_\lambda(x) = \sum_{n=0}^{\infty} \frac{e^{-\lambda}\,\lambda^n}{n!} \frac{e^{-\frac{(x-n)^2}{2\sigma_n^2}}}{\sigma_n\sqrt{2\pi}} \tag{A.4}$$

with a variance of

$$\sigma_n^2 = n\left(F^2 - 1\right) + \sigma_{el}^2 \tag{A.5}$$

σ_0^2 is the variance of the pedestal which is equal to the electronic noise contribution $\sigma_0^2 = \sigma_{el}^2$. A consistency crosscheck of the output distribution function $f_\lambda(x)$ to the definition of the excess noise factor can be found in Appendix A.

The variance of the electronic noise σ_{el} in the case of the CT1 camera electronics is estimated to be equivalent to 0.5 PhE. The excess noise is **typically** approximately $F^2 = 1.3$.

A very important point that has to be taken into account is that the output of the PMTs is coupled to the transimpedance amplifier via a **capacitance** such that only fast pulses are
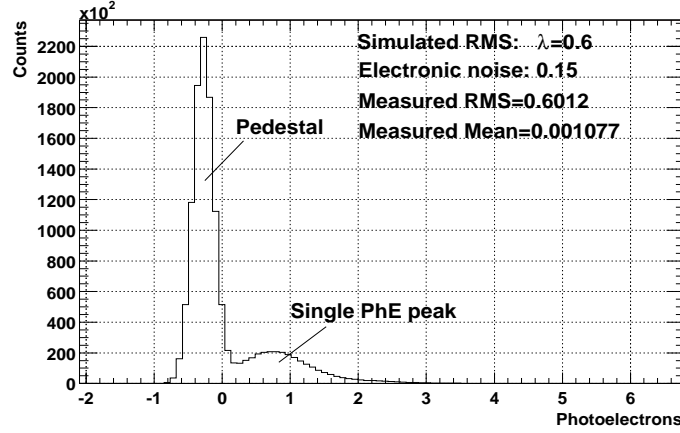
Figure A.1: This plot shows the simulation of the night sky background. Here the electronic noise was set to only 0.15 PhE in order to be able to see the single PhE peak.

amplified. **Only the fluctuations** of the DC like NSB are amplified. Therefore the average has to be subtracted:

$$f_{LONS}(x) = f_\lambda(x) - \lambda \tag{A.6}$$

$f_{LONS}(x)$ is the final simulated night sky background (NSB). Fig. A.1 shows a simulated NSB with a total RMS of 0.6 PhE. Here the electronic noise was set to only 0.15 PhE in order to be able to see the single PhE peak.

For subsequent data analysis an electronic noise of 0.5 PhE was used which corresponds to the estimated electronic noise of the CT1 camera read-out.

In order to treat the night sky background correctly, the pedestal distributions for each pixel are simulated on top of the MC shower images according to the measured pedestal RMS of the recorded data run. Since the starfield changes from object to object and the night sky background depends strongly on the zenith angle, the night sky background is simulated differently for each dataset. For the optimization of cuts or the training of the LDA it is very important to divide the recorded data into zenith angle bins and simulate the NSB **exactly with the same zenith angle distribution** on top of the MC shower images because the NSB depends on the zenith angle, which will be shown later. Within each zenith bin angle the available events are distributed in equal numbers among the recorded runs. Then for each run the pedestal information is taken and the NSB is simulated accordingly. By this procedure it has been **ensured** that the night sky background of the MC showers resembles as much as possible the NSB in the recorded data **with the same zenith angle distribution**.

Finally, after our gamma data sample has been prepared to be comparable to the recorded data set and selection cuts have been applied, we are interested in determining the flux.

A.2.2   Trigger efficiencies, cut efficiencies and effective areas

The fluxes seen by the telescope have to be calculated out of the measured **event rate** and the **efficiencies** of the telescope. In general the **differential flux** is defined as

$$\frac{dF}{dE} = \frac{dN}{dE\,dA\,dt} \tag{A.7}$$

Where F is the flux, E is the energy, A is the area, N is the number of particles (γ's) and t is the time. The telescope **efficiencies** are defined as the ratio of the number of so-called

excess events N_{Excess} and the real existing number of events N_{Real}.

$$\varepsilon_{tot} = \frac{dN_{Excess}}{dN_{Real}} \tag{A.8}$$

The **excess events** $N_{Excess} = N_{Pass} - N_{Back}$ are the measured events by the telescope which passed the γ-selection cut minus the background events. The efficiencies of the telescope can only be obtained by **MC simulation** since we do not have a test beam with cosmic γ's. Thus, the **efficiencies** are defined as the **ratio** of the events that passed the γ-selection cut $N_{Selected}(E, \theta, r)$ and the total simulated events $N_{Simulated}(E, \theta, r)$.

$$\varepsilon_{Total}(E, \theta, r) = \frac{dN_{Selected}(E, \theta, r)}{dN_{Simulated}(E, \theta, r)} \tag{A.9}$$

The number of events that passed the selection cut (selection efficiencies) are **dependent** on the **energy** E, the **zenith angle** θ and the **impact parameter** r. The total efficiency and can be split into **two parts**, the trigger efficiency of the telescope trigger electronics and the cut efficiency of the selection cut (in the data analysis):

$$\varepsilon_{Total}(E, \theta, r) = \varepsilon_{Trigger}(E, \theta, r) \cdot \varepsilon_{cut}(E, \theta, r) \tag{A.10}$$

The best way to **introduce** the **concept of effective areas** $A_{eff}(E, \theta, r)$ is by **calculating** the excess events out of the **flux:**

$$
\begin{aligned}
\frac{dN_{Excess}}{dE} &= \int \frac{dF}{dE} \varepsilon_{Total}(E, \theta, r) \; dt \, dA \\
&= \frac{dF}{dE} \sum_{\theta_i} T_{obs}^{\theta_i} \int \int \varepsilon_{Total}(E, \theta_i, r) \; dr \, d\phi \\
&= \frac{dF}{dE} \sum_{\theta_i} T_{obs}^{\theta_i} A_{eff}(E, \theta_i)
\end{aligned}
\tag{A.11}
$$

The integral over the time has been transformed into a sum over zenith angle bins θ^i because the effective areas depend on the zenith angle and a binning of the recorded telescope data into zenith angle bins is unavoidable. The integration over the impact area has been separated into an integration over the radius r (rotational symmetry) and the azimuth angle ϕ.

The **effective area** is therefore the integral over the efficiencies (which are obtained from MC studies):

$$
\begin{aligned}
A_{eff}(E_k, \theta_l) &= \int \int \varepsilon_{Total}(E_k, \theta_l, r) \; d\phi dr \\
&= 2\pi \int_0^\infty \varepsilon_{Total}(E_k, \theta_l, r) \; dr \\
&= \pi \sum_{i=1}^N \frac{N_{Selected}(E_k, \theta_l, r_i)}{N_{Simulated}(E_k, \theta_l, r_i)} \left(r_{up}^2(i) - r_{low}^2(i) \right)
\end{aligned}
\tag{A.12 / A.13}
$$

The effective area **depends** on the **energy** and the **zenith angle** (see Fig. A.2). $r_{up}(i)$ and $r_{low}(i)$ are the upper and lower edge of the impact parameter bin i, respectively. A **binning** in impact parameter, energy and zenith angle is **unavoidable.** As above $N_{Selected}(E_k, \theta_l, r_i)$ is the number of events in the according energy/zenith angle/impact parameter-bin that passed the selection cut and $N_{Simulated}(E_k, \theta_l, r_i)$ is the number of events that have been simulated originally for the same bin.

The effective areas are also slightly dependent on the shape of the flux spectrum because of the binning in energy bins. In order to avoid systematic errors, each MC event is weighted with $W(E)$ in such a way that the weighted MC distribution forms the desired spectrum. The desired spectrum should be similar to the spectrum of the source that is measured. This can be achieved by an iterative process for which the measured spectrum is placed back into the effective area calculation. The systematic error here is reduced when taking small energy bins. The weights are normalized to one.

The **effective area** is the conversion factor from the **excess event rate** to **gamma ray flux** which is calculated in the following way:

$$\frac{dF}{dE} \quad = \quad \frac{\frac{dN_{Excess}}{dE}}{\sum_{\theta_i} T_{obs}^{\theta_i} A_{eff}(E, \theta_i)} \tag{A.14}$$

The errors on the fluxes are calculated via Gaussian error propagation from errors on N_{excess} and A_{eff}. The errors on the effective areas are statistical Poissonian fluctuations from $N_{selected}^i$ and from $N_{Simulated}(E, \theta, r_i)$ and they add up quadratically:

$$\sigma_{A_{eff}}^2 = \pi \sum_{i=1}^{N} \left[\frac{\sqrt{N_{selected}(E, \theta, r_i)}}{N_{Simulated}(E, \theta, r_i)} \left(r_{up}^2(i) - r_{low}^2(i) \right) \right]^2 \tag{A.15}$$

A.3   Gamma/hadron separation methods

For this analysis I used an approach which first describes the shower image by using **so-called image parameters**. The distributions of the image parameters for γ's and hadrons exhibit some differences. A cut method which uses these differences separates the two event types using image parameters was developed. Another approach, which has not been used in this thesis, is to directly apply a **maximum-likelihood fit** to the shower images themselves [CAT89]. This approach depends on how well it is possible to model the shape of gamma showers and hadronic showers which need to be used as templates for the fit.

In this section I wish to introduce as a first step the classical image parameters, called '**Hillas parameters**' which are named after A. Hillas who invented them in 1985 [Hil85]. Afterwards, simple static cuts and a linear discriminant analysis (LDA) will be described. Eventually the LDA will be used mainly as a tool to quantify the discrimination power of different image parameter sets as it increases in discrimination power of a given parameter set, compared to the static cuts.

A.3.1   The classical Hillas parameters to describe shower images

As shown in chapter 1, concerning theory and detectors, the main differences between **gamma photon initiated** showers and **hadron initiated showers** lie in their **geometrical** structure and, to a lesser extend in their time structure (which is not discussed in this thesis). Due to the longer interaction length of the hadronic interaction, the **hadronic showers** show **more fluctuations** in their image than do the electromagnetic showers. In addition, hadronic showers have a **wider lateral distribution**. Therefore, A. Hillas therefore proposed to calculate the geometrical variances of the shower image which are different for hadronic and gamma showers. He introduced the first and second moments of the shower image. In the following, I describe a form with **generalized weights** w_i which will be used later on (where x_i and y_i are the coordinates of pixel i). In case of the classical Hillas parameters, the weight w_i is the charge collected by pixel i in photoelectrons $w_i = q_i$. Fig. A.3 illustrates the geometric meaning of the image parameters.
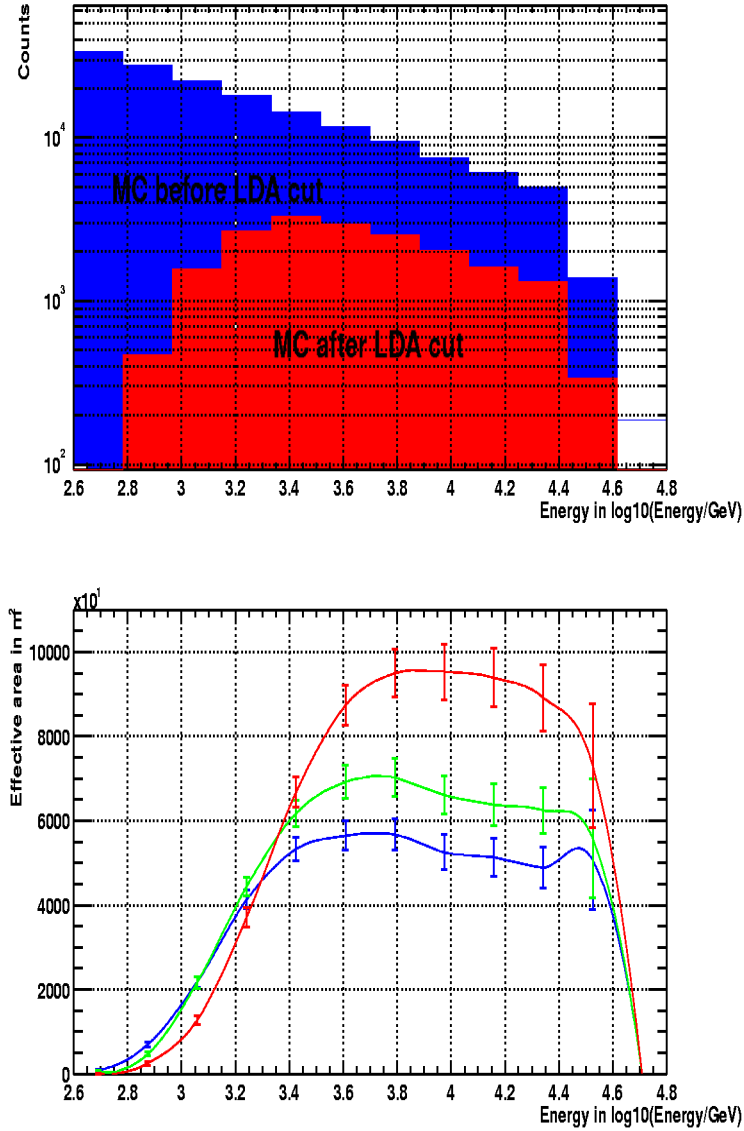
The **first moments** are

Figure A.2: The upper plot shows the **total simulated MC event distribution** (blue histogram) and the **events that passed the selection cut** (red curve), integrated over all impact parameters. The lower plot shows the **effective areas** for the selection cuts developed in this thesis using a power-law spectrum with spectral index $\alpha = -2.8$. The three curves represent the effective areas for **three** zenith angles: $12°$ (blue), $32°$ (green) and $50°$ (red).
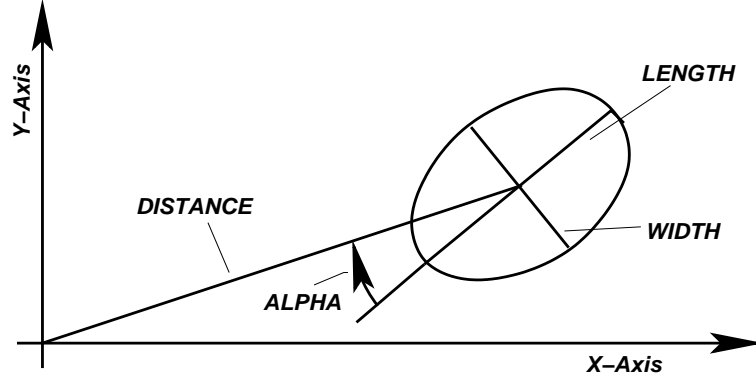
Figure A.3: An illustration of the geometric meaning of the image parameters.

$$\langle x \rangle \quad = \quad \frac{\sum_{i=1}^{N} x_i w_i}{\sum_{i=1}^{N} w_i} \tag{A.16}$$

$$\langle y \rangle \quad = \quad \frac{\sum_{i=1}^{N} y_i w_i}{\sum_{i=1}^{N} w_i}$$

and the **second moments**

$$\langle x^2 \rangle \quad = \quad \frac{\sum_{i=1}^{N} x_i^2 w_i}{\sum_{i=1}^{N} w_i} \tag{A.17}$$

$$\langle y^2 \rangle \quad = \quad \frac{\sum_{i=1}^{N} y_i^2 w_i}{\sum_{i=1}^{N} w_i}$$

$$\langle xy \rangle \quad = \quad \frac{\sum_{i=1}^{N} x_i y_i w_i}{\sum_{i=1}^{N} w_i}$$

The **variances** can be calculated in the classical way:

$$var(x^2) \quad = \quad \langle x^2 \rangle - \langle x \rangle^2 \tag{A.18}$$

$$var(y^2) \quad = \quad \langle y^2 \rangle - \langle y \rangle^2$$

$$covar(xy) \quad = \quad \langle xy \rangle - \langle x \rangle \langle y \rangle$$

The variances can be put together to form the so-called **covariance matrix**

$$M = \begin{pmatrix} var(x^2) & covar(xy) \\ covar(xy) & var(x^2) \end{pmatrix} \tag{A.19}$$

The covariance matrix can be used to describe a **two dimensional Gaussian distribution** function

$$G(x,y) \quad = \quad \frac{1}{\sqrt{(2\pi)^2 \det M}} e^{-\frac{1}{2} \mathbf{u} M^{-1} \mathbf{u}} \tag{A.20}$$

$$\mathbf{u} M^{-1} \mathbf{u} \left(1 - \rho^2\right) \quad = \quad \frac{u_1^2}{var(x^2)} - 2\rho \frac{u_1 u_2}{\sqrt{var(x^2)\, var(y^2)}} + \frac{u_2^2}{var(y^2)}$$

with the **correlation coefficient**

$$\rho = \frac{covar(xy)}{\sqrt{var(x^2)\,var(y^2)}} \tag{A.21}$$

and

$$\begin{aligned} u_1 &= x - \langle x \rangle \\ u_2 &= y - \langle y \rangle \end{aligned} \tag{A.22}$$

The two dimensional Gaussian distribution is **rotated** in the camera coordinate system by an angle given by

$$\tan 2\phi = 2\frac{covar(xy)}{var(x^2) - var(y^2)} \tag{A.23}$$

By **diagonalizing the matrix** M, one obtains the longitudinal (LENGTH) and the lateral (WIDTH) variances of the shower image. By introducing the helper variables

$$\begin{aligned} d &= var(y^2) - var(x^2) \\ z &= \sqrt{d^2 + 4covar^2(xy)} \\ u &= 1 + \frac{d}{z} \\ v &= 2 - u \\ w &= \langle x \rangle^2 \langle y^2 \rangle - 2 \langle x \rangle \langle y \rangle \langle xy \rangle + \langle y \rangle^2 \langle x^2 \rangle \end{aligned} \tag{A.24}$$

WIDTH and **LENGTH** can be defined can be defined as:

$$WIDTH = \sqrt{\frac{var(x^2) + var(y^2) - z}{2}} \tag{A.25}$$

$$LENGTH = \sqrt{\frac{var(x^2) + var(y^2) + z}{2}} \tag{A.26}$$

Additional **useful image parameters** include:

$$DIST = \sqrt{\langle x \rangle^2 + \langle y \rangle^2} \tag{A.27}$$

$$AZWIDTH = \frac{\sqrt{w}}{DIST} \tag{A.28}$$

$$MISS = 0.5\left(u\langle x \rangle^2 + v\langle y \rangle^2\right) - \frac{2covar(xy)\langle x \rangle \langle y \rangle}{z}$$

$$ALPHA = \arcsin\frac{MISS}{DIST} \tag{A.29}$$

$$m_{ax} = \frac{d + \sqrt{d^2 + 4covar(xy)^2}}{2covar(xy)}$$

$$m_{ce} = \frac{\langle x \rangle}{\langle y \rangle}$$

$$pr = m_{ax}m_{ce} \tag{A.30}$$

$$SIGN = \begin{cases} 1 \, if \, (pr \geq 0) \, \& \, (m_{ax} \geq m_{cer}) \\ -1 \, if \, (pr \geq 0) \, \& \, (m_{ax} < m_{ce}) \\ 1 \, if \, (pr < 0) \, \& \, (m_{ax} \leq \frac{1}{m_{ce}}) \\ -1 \, if \, (pr < 0) \, \& \, (m_{ax} > \frac{1}{m_{ce}}) \end{cases} \tag{A.31}$$
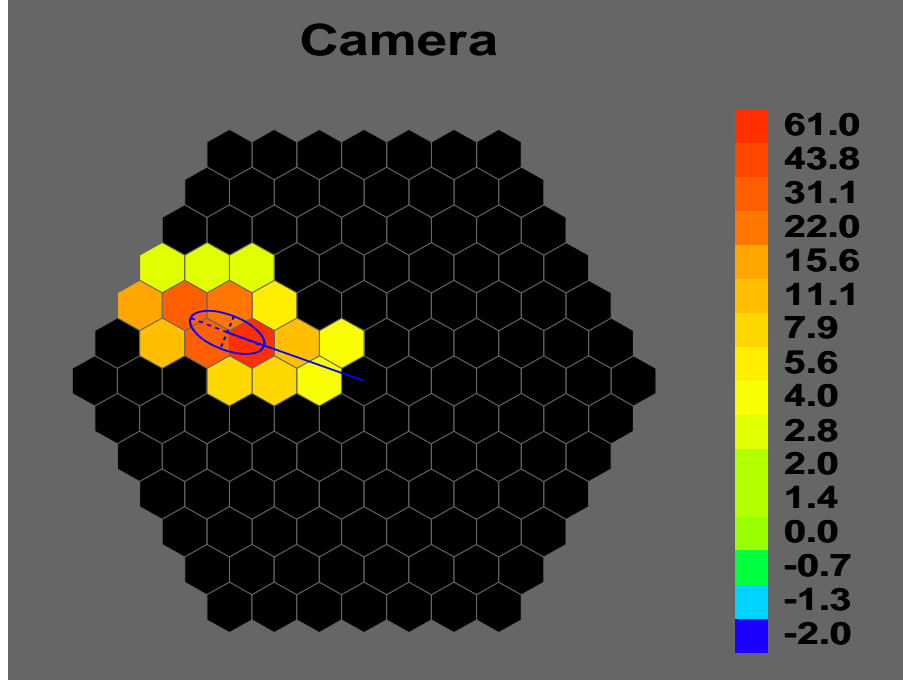
Figure A.4: The CT1 camera with a simulated gamma shower with its Hillas ellipse after image cleaning.

$$SIZE \quad = \quad \sum_{i=1}^{N} q_i \qquad\qquad (A.32)$$

$$CONC \quad = \quad \frac{q_{1.} + q_{2.}}{SIZE} \qquad\qquad (A.33)$$

where **DIST** (Equ. A.27) is the distance from the camera center to the center of gravity of the shower in degrees and it depends on the energy, the impact parameter and the zenith angle of the γ (see section 1.4.1 and Fig. A.3).

AZWIDTH (Equ. A.28) has not been used in this thesis because it does not improve the discrimination power anymore.

ALPHA (Equ. A.29) is the most important cut parameter for point sources. It is defined as the clockwise angle from the longitudinal axis of the shower to the connection line between the center of the camera and the shower center of gravity. Since the center of the camera of the telescope usually points towards the point source itself, the shower axis of gamma showers points toward the center. Conversely, hadronic showers arrive from all directions and the distribution is flat for all angles for an infinitely large camera (for a finite size camera the ALPHA distribution is no longer uniform). Equ. A.29, shown above, gives values between $0°$ and $90°$. ALPHA defines an angle between $0°$ and $180°$ or equivalently, from $-90°$ to $+90°$. For some calculations **the sign of ALPHA is needed**. It can be obtained from Equ. A.31.

Another very basic parameter is **SIZE** (Equ. A.32). This is simply the total charge collected in units of photoelectrons (PhE). It is the **main estimator for the energy**, but depends also strongly on the zenith angle of the source and the impact parameter.

CONC (Equ. A.33) is the ratio of the sum of the two highest pixel charges to the total charge. Gamma showers have a smaller lateral and longitudinal electron distribution and peak more in the center of the image, in contrast to hadronic showers.

Therefore, **CONC** is bigger and **WIDTH** and **LENGTH** are **smaller** for gamma showers than for hadronic showers (see Fig. A.5). Since the camera of CT1 has rather
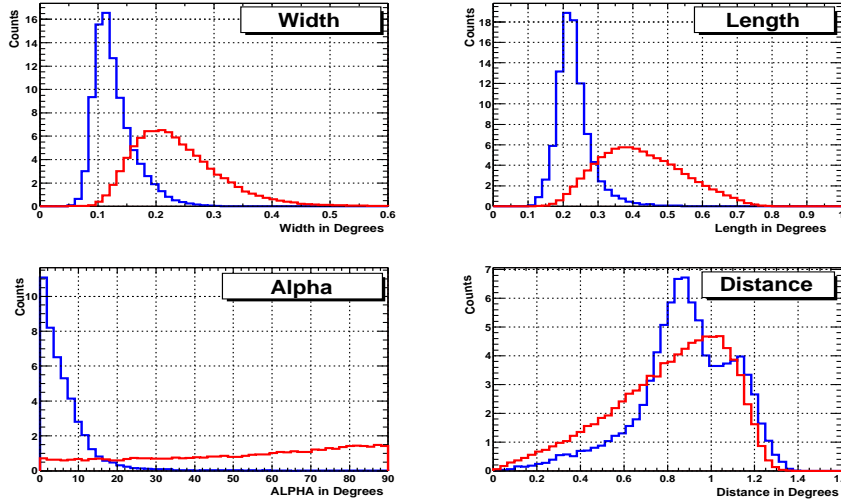
Figure A.5: The distributions of the four most important image parameters: WIDTH, LENGTH, ALPHA and DISTANCE . MC gammas are blue and recorded off-data is red.

large pixels (0.25° diameter), CONC is not very smoothly defined and shows a rather large spread. The following two figures show a) a ***typical gamma shower image*** with applied tail cut (see section about image cleaning) in the CT1 camera (Fig. A.4) and b) the ***distributions*** of the ***four most important*** image parameters (Fig. A.5). The second hump in the DIST distribution results from shower images that where larger than the radius of the camera and were therefore cut at the camera border (see leakage parameter). A selection cut of SIZE > 100 photoelectrons (PhE) has been applied.

Expression A.20 can be used to define a so-called ***covariance ellipse***, a line of equal probability, of 1 sigma (defined by WIDTH, LENGTH, DIST and ALPHA), around the center of weight. It is the so-called ***Hillas ellipse***. It is a description of the shower image (see Fig. A.4).

The definition of the image variances given above assumes that there is no noise background in the image. Unfortunately, this is never the case because we have NSB as we know. In Equ. A.17 it can be seen that the distance of the pixels enters as a square in the sum and, consequently, the calculation of the variances of the shower image gives entirely incorrect values. Therefore, an image cleaning (sometimes called a tail-cut), becomes necessary to remove, at least in part, the effect of the NSB.

A.3.2 Image cleaning algorithms to remove the night sky background in the camera

The image cleaning (or tail cut) ***removes*** the night sky background (NSB) in the camera. Without this it would not be possible to calculate the image variances, as explained above. Traditionally a dynamical image cleaning has been used [Pet97]. The RMS values of the pixels are measured in independent pedestal runs and the signal of the pixels are compared to their RMS values in order to decide if the pixels should be included in the parameter calculation or not.

In this analysis ***three different algorithms*** have been tested. In all three cleaning methods two cleaning parameters were introduced: The '***image core limit***' κ_c and the '***image border limit***' κ_s.

The 'classical' cleaning method

1. All pixels that have a signal ***larger*** than κ_c (image core limit) times the Pedestal RMS ***are retained.***

2. All pixels that have a signal ***larger*** then κ_s (image border limit) times the Pedestal RMS are retained ***if*** they have a neighbour with more than κ_c sigma.

3. Single pixels are ***removed*** if the signal is ***smaller*** than 5 times the Pedestal RMS.

The 'island' cleaning method

First, the 'classic' cleaning algorithm is applied. Afterwards, the image is being analyzed for ***islands*** (islands are isolated clusters of pixels which remain after a classical cleaning. The meaning of 'island' is illustrated in Fig. A.24.). Only the ***largest*** island (in terms of charge; this is the main shower image) ***is retained***, all the others are removed. The island finding algorithm is explained in detail in the section concerning mountains and islands.

The 'mountain' cleaning method

The method is based on the ***quantification of fluctuations*** in the shower image, which are different for hadronic showers and electromagnetic showers.

In the first step, the 'classical' image cleaning is again applied. Then a complex image structure analysis is performed with respect to the ***'mountain' structure*** (The meaning of 'mountain' is illustrated in Fig. A.24.) of the image. This will be described in detail in section A.4 where new image parameters are introduced. In a recursive procedure the image is divided into mountains. (The analogy of mountains or valleys is with respect to their signal content). The ***cut lines are the valleys*** between the mountains. The charge in each cluster (mountain) is summed up and the ***largest mountain is retained*** while the others are cleaned away.

Later, these three algorithms will be compared with each other, with respect to their capability of delivering the best image parameters.

General comments

Dynamical[3] image cleaning procedures have the advantage of ***retaining as much as possible*** of the image in order to have the ***largest*** amount of information about the shower available. On the contrary, 'dynamical' cleaning procedures also have some ***disadvantages*** compared to fixed level image cleaning methods. When the tail-cut becomes ***dependent*** on the pedestal RMS, which is actually a measure of the NSB and the starlight, then as a consequence, the values for WIDTH and LENGTH ***also*** become ***dependent*** on the NSB. In other words, WIDTH and LENGTH will change at different night sky and weather conditions and dependencies that have not been there before are artificially introduced into the analysis.

A.3.3   Static cuts and dynamical cuts: Dependence of the Hillas parameters on the energy, the zenith angle, the impact parameter and the night sky background

Having introduced the parameters that describe the shower image we now wish to use them for hadronic background ***suppression***. In the following section the image parameters have been calculated in the classical way with weights $w_i = q_i$.

---

[3]The expression 'dynamical' is understood in the sense that the cleaning level is chosen as a function of the NSB (pedestal RMS).

Static cuts and the optimization of cut intervals

The simplest method for gamma/hadron separation consists of a *static cut* on the image parameter values. These cuts are commonly called *super cuts* (Wipple collaboration, Ref. [Rey93]). The following values have been obtained by following the procedure described below and using a data set of Mkn 421 (flares Feb 8/9, 2001):∘

$$
\begin{aligned}
0.05° &\leq WIDTH \leq & 0.11° \\
0.1° &\leq LENGTH \leq & 0.42° \\
0° &\leq ALPHA \leq & 12° \\
0.31° &\leq CONC \leq & 0.7° \\
0.5° &\leq DIST \leq & 1.0°
\end{aligned}
\tag{A.34}
$$

The *cut on ALPHA* is a geometrical cut and only works for *point sources*. The lower cut on DIST is applied because images with too small impact parameters yield showers that are too round and too close to the center of the camera (bad definition of ALPHA) which makes a discrimination impossible. The upper limit is used to remove showers that are excessively affected by a limited camera size and that are truncated at the border.

The *cut efficiencies* for γ's: $\varepsilon_G = N_C^G/N_{tot}^G$ and hadrons: $\varepsilon_H = N_C^H/N_{tot}^H$ describe the percentage of events that have been selected after application of the cuts on simulated MC events. N_{tot}^H and N_{tot}^G are the number of all triggered γ-events and hadron-events. They have been simulated with a certain spectral index (power law, spectral index α=1.5) . The quantity ε_G should be as large as possible, usually at least 50 %, and ε_H should be as small as possible. Usually it is 0.5 % (Background reduction factor 200). The *quality factor* is defined by

$$
Q = \frac{\varepsilon_G}{\sqrt{\varepsilon_H}}
\tag{A.35}
$$

It is a measure of how well the background has been *suppressed* by keeping enough signal events. Typical values for the static cut are about *seven*.

The algorithm for *cut interval optimization* changes the intervals in small systematic steps in order to maximize either the *quality* factor or the *significance* (applied to pure MC-samples). The significance is the signal to noise ratio:

$$
\begin{aligned}
S &= \frac{N_{on} - N_{off}}{\sqrt{N_{on} + N_{off}}} \\
&= \frac{N_C^G}{\sqrt{N_C^G + 2N_C^H}}
\end{aligned}
\tag{A.36}
$$

where $N_{on} = N_C^G + N_C^H$ and $N_{off} = N_C^H$ for Monte Carlo samples. S converges to

$$
S \to Q\sqrt{N_{tot}^G}
\tag{A.37}
$$

for

$$
N_C^G \gg N_C^H
\tag{A.38}
$$

Unfortunately, the quantity N_C^G is usually rather of the same order as N_C^H which means Equ. A.38 is not fulfilled and as a consequence, the optimization of the quality will *not* optimize the significance. That implies that it is *more appropriate to optimize on the significance* Equ. A.36, rather than on the quality Equ. A.35.

Further, if the significance is used for cut optimization then ratio N_{tot}^G/N_{tot}^H (if applied to MC samples) has to have the *same value* of approximately 0.005 which is observed in nature.
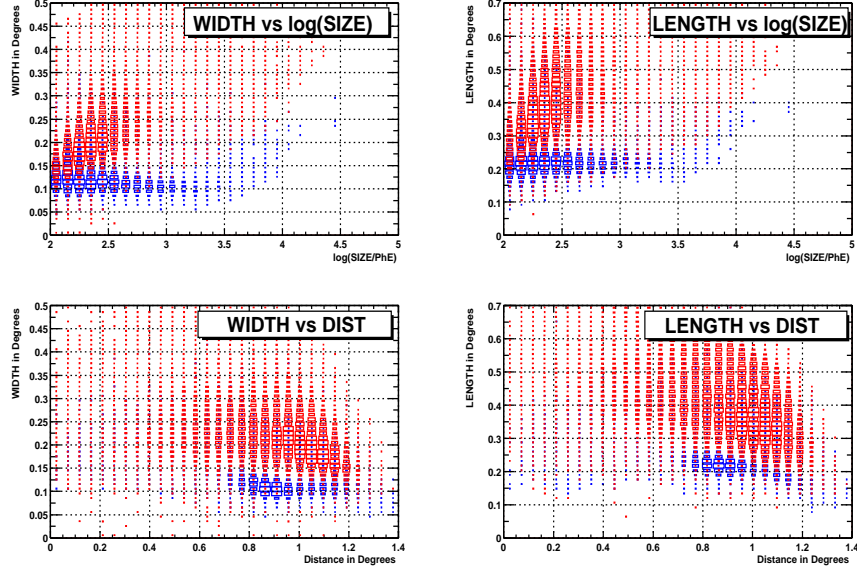
Figure A.6: The dependence of the parameters WIDTH and LENGTH **on** SIZE and DIST. MC gamma distribution is blue and recorded off-data is red.

The significance as defined above Equ. A.36 is **not Gaussian distributed** and is therefore not appropriate to estimate the **probability**. This is important if one would like to claim a discovery with a small significance. An expression for the significance with Gaussian distribution has been defined by [LiMa83] as a log-likelihood ratio.

$$
S = \sqrt{2} \left\{ N_{on} \ln \left[\frac{1+\alpha}{\alpha} \left(\frac{N_{on}}{N_{on+N_{off}}} \right) \right] + \right. \tag{A.39}
$$

$$
\left. N_{off} \ln \left[(1+\alpha) \left(\frac{N_{off}}{N_{on} + N_{off}} \right) \right] \right\}^{\frac{1}{2}}
$$

where $\alpha = \frac{T_{ON}}{T_{OFF}}$ is the ratio of the observation times of the off-data sample and the on-data sample. This form of calculating the significance has been used **in this analysis**.

By experience it has been found that the optimization on the quantity

$$
P = S \cdot \sqrt{N_{ON} - N_{OFF}} \tag{A.40}
$$

yields good results, because it forces the optimization algorithm to not only maximize the significance but to also keep a reasonable number of excess events $N_{Ex} = N_{ON} - N_{OFF}$.

The maximization procedure is nontrivial because each variation of a cut changes the sample and also because the data distribution has statistical fluctuations. The algorithm has to be able to handle these obstacles. The results of most algorithms **depend on the initial value** and are **not reproducible**, only within a certain range and error. The result also varies slightly with small changes in the training data sample. This also pertains to dynamical cuts which are described in the following paragraph.

The optimization of dynamical cuts

The values of WIDTH, LENGTH, SIZE, DIST and CONC depend not only on the **night sky background** (expressed in pedestal RMS values) but also on the **energy** (estimator SIZE), the **impact parameter** (estimator DIST) and the **zenith angle** of the object in the sky (which is known and measured during the run).